

[Article]

www.whxb.pku.edu.cn

pH 值对十二胺在碳钢表面的吸附行为及缓蚀机理的影响

鲁照玲 邱于兵 郭兴蓬*

(华中科技大学化学化工系, 湖北省材料化学与材料服役失效重点实验室, 武汉 430074)

摘要: 采用电化学方法和扫描电镜技术, 研究了 pH 值对十二胺在碳钢表面的吸附以及对碳钢 CO₂ 腐蚀缓蚀机理的影响。研究表明, 溶液的 pH 值对十二胺的吸附和缓蚀机理起决定性作用。十二胺对碳钢的缓蚀作用随溶液 pH 值的增加而增强。pH 值为 4.9 时, 十二胺主要抑制腐蚀的阴极过程。缓蚀剂分子在金属表面上的吸附能比较低, 缓蚀剂容易发生脱附, 因此不能有效抑制腐蚀反应的进行。pH 值为 6.9 时, 缓蚀剂的吸附能较高, 能够牢固地吸附在金属表面, 形成有效的扩散阻挡层, 同时抑制腐蚀的阴、阳极过程, 从而有效地抑制腐蚀反应的进行。

关键词: 二氧化碳; 十二胺; 吸附; 缓蚀机理; pH 值; 碳钢

中图分类号: O646

Effect of pH Value on the Adsorption Behavior and Inhibition Mechanism of Dodecylamine on Carbon Steel

LU Zhao-Ling QIU Yu-Bing GUO Xing-Peng*

(Key Laboratory of Materials Chemistry and Service Failure of Hubei Province, Department of Chemistry and Chemical Technology, Huazhong University of Science and Technology, Wuhan 430074, P. R. China)

Abstract: The effect of pH value on the adsorption behavior and inhibition mechanism of dodecylamine for carbon dioxide corrosion of carbon steel was investigated by electrochemical methods and scanning electron microscopy (SEM). The results indicated that the pH value of the solution played the crucial role to the adsorption behavior and inhibition mechanism of dodecylamine. The inhibition performance of dodecylamine on carbon steel was dependent on the pH value and the inhibition efficiency increased with the increase of pH value. At pH 4.9, dodecylamine mainly inhibited the cathode process of the corrosion. The adsorption energy of dodecylamine on the metal surface was lower. The adsorption of dodecylamine on the metal surface was not stable and an anode desorption phenomenon could be observed. Hence, dodecylamine did not provide effective inhibition to the corrosion. While at pH 6.9, it had much higher adsorption energy. Dodecylamine adsorbed on the metal surface tightly and formed the effective diffusion barrier which inhibited both the cathode and anode processes effectively.

Key Words: Carbon dioxide; Dodecylamine; Adsorption; Inhibition mechanism; pH value; Carbon steel

The change of metal surface states with pH value of solutions not only has influence on the corrosion behavior of the metal, but also can effect significantly on the adsorption stability and inhibition mechanism of inhibitors^[1,2]. The results of the statistical analysis by Hernandez *et al.*^[3] have shown that pH value after the flow velocity was the most important factor that influ-

enced the corrosion rates of the steel in the conditions when adding inhibitors. In the practical produced water of oil fields, the alkaline ions HCO₃⁻ can make up buffered solutions with the dissolved CO₂ and hence made the aqueous solution in near neutral environment. There are two distinct characteristics of the aqueous solution containing CO₂ in near neutral environment:

Received: July 12, 2007; Revised: October 23, 2007; Published on Web: January 4, 2008.

English edition available online at www.sciencedirect.com

*Corresponding author. Email: guoxp@mail.hust.edu.cn; Tel/Fax: +8627-87543432.

国家自然科学基金(50471062)资助项目

one is that the solution is rich in HCO_3^- ($\text{pH} > 6.8$, 99% HCO_3^-)^[4]; the other is that FeCO_3 has large tendency to crystallize and hence it can cause the dramatic change of the surface state. Much work about the performance evaluation and inhibition mechanism of inhibitors was carried out in CO_2 -saturated acidic aqueous solution (pH 3.9 at room temperature^[5]), and it was still lack of systematic investigation about the adsorption behavior and inhibition performance of inhibitors in near neutral environments. The selection and application of inhibitors are environment-dependent, that is the inhibitor which behaves well in acidic environment might have no role in near neutral environment and vice versa. No doubt that the investigation of inhibition behavior in near neutral environments will contribute to the understanding of the inhibition mechanism of inhibitors in near neutral environments and hence might give guidance to the effective selection and successful design of new inhibitors in near neutral environment.

The nitrogen-containing inhibitors, especially the imidazoline-based inhibitors, have been widely used in oil fields to prevent carbon dioxide corrosion. Although much study has done as to the inhibition mechanism, no consistent conclusion was made up to date. The complexity of the components of the commercial inhibitors and the increase of the hydrolyzation trend of imidazoline with pH increase do no favor to the investigation of the inhibition mechanism. Hence, dodecylamine with the simple molecule structure was considered as the model inhibitor in this study. The electrochemical and surface analysis methods were adopted to investigate the adsorption behavior and inhibition mechanism of dodecylamine at different pH values, and further to probe the influence of pH value on the inhibition performance of dodecylamine on N80 steel.

1 Experimental

1.1 Test conditions and materials

All the electrochemical experiments were carried out using a three-electrode cell of 500 mL with a condenser on the top of the bubbling tube to keep the solution concentration stable in the test temperature. The auxiliary electrode was platinum foil. A saturated calomel electrode (SCE) was used as the reference. The chemical compositions of N80 steel as the working electrode are shown in Table 1. The electrode was embedded in the epoxy resin (exposed surface area 0.785 cm^2) mechanically polished with 180#, 320#, 600#, 1000#, and 1200#, rinsed with the distilled water and degreased with acetone.

Test solution was prepared using the distilled water, and analytical grade reagents: sodium chloride and sodium bicarbonate. The sodium bicarbonate was used to adjust pH value of the solution. The dodecylamine used in this experiment was provided by

Table 1 Chemical compositions of N80 steel

$w(\text{C})$ (%)	$w(\text{Si})$ (%)	$w(\text{Mn})$ (%)	$w(\text{P})$ (%)	$w(\text{S})$ (%)
0.38–0.45	0.15–0.35	1.55–1.85	≤ 0.025	≤ 0.025
$w(\text{Cr})$ (%)	$w(\text{Ni})$ (%)	$w(\text{Cu})$ (%)	$w(\text{Mo})$ (%)	$w(\text{Fe})$ (%)
<0.20	<0.20	<0.20	0.15–0.25	bal.

Arcos Organics, USA. The solution was saturated by CO_2 up to 6 h before the electrochemical measurements to keep pH value stable. The test temperature was controlled thermodynamically at $(50.0 \pm 1.0) ^\circ\text{C}$.

1.2 Electrochemical measurements

The potentiodynamic polarization was carried out using the Corrtest system and the scanning rate was $0.5 \text{ mV} \cdot \text{s}^{-1}$ starting from -150 mV to $+150 \text{ mV}$ (*vs* open circuit potential, E_{oc}). The electrochemical impedance spectroscopy (EIS) was carried out using IM6e system. The working electrode was stabilized in CO_2 -saturated 3% (*w*) NaCl solution for about 1 h at the open circuit potential (E_{oc}), the cathode polarization potential (-50 mV *vs* E_{oc}) and the anode polarization potential ($+50 \text{ mV}$ *vs* E_{oc}), respectively. Zview software was used to fit the experimental impedance data according to the chosen equivalent circuit.

1.3 Surface analysis

The specimens were immersed in CO_2 -saturated 3% NaCl solution without or with dodecylamine for 24 h. After the immersion, the specimens were rinsed by the deoxygenated water to remove the impurities adsorbed on the metal surface and then were stored in the desiccator impregnated with N_2 . Scanning electron microscopy (SEM, QUANTA 200, FEI) was used to obtain the information about the morphology characteristics of the metal surface in the absence or presence of dodecylamine.

2 Results and discussion

2.1 Potentiodynamic polarization

Fig.1 shows the potentiodynamic polarization curves of N80

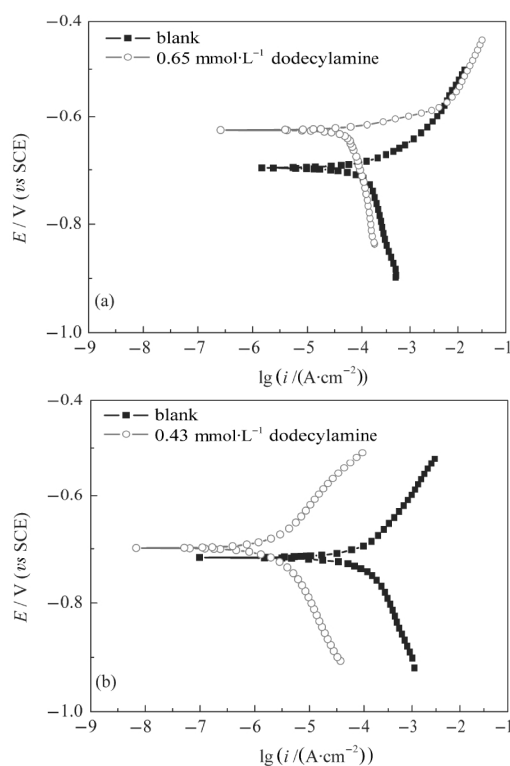


Fig.1 Polarization curves of N80 electrode in CO_2 -saturated 3% NaCl solution without or with dodecylamine

(a) $\text{pH}=4.9$; (b) $\text{pH}=6.9$

Table 2 Parameters for N80 electrode in CO₂-saturated 3% NaCl solution without and with dodecylamine

pH	c(dodecylamine) (mmol·L ⁻¹)	E_{corr} mV	b_a mV	b_c mV	i_{corr} ($\mu\text{A}\cdot\text{cm}^{-2}$)	$\eta(\%)$
4.9	0.00	-697	56	306	141	-
	0.65	-627	27	489	69	51.2
6.9	0.00	-716	104	219	74	-
	0.43	-699	134	223	2.1	97.2

E_{corr} is the corrosion potential of N80 steel; b_a and b_c are the Tafel slopes of anode and cathode, respectively; i_{corr} is the fitted corrosion current density of N80 steel; η is the inhibition efficiency of dodecylamine on N80 steel.

electrode in CO₂-saturated 3% NaCl solution at pH 4.9 and 6.9 without or with dodecylamine. The electrochemical parameters and the corrosion rate fitted with the method of three parameters in the weak polarization region are presented in Table 2. E_{corr} is the fitted corrosion potential of N80 steel; b_c and b_a are the cathodic and anodic apparent Tafel slopes, respectively; i_{corr} is the corrosion current density. The inhibition efficiency (η) of dodecylamine on N80 steel was calculated by the following equation:

$$\eta = (1 - i'_{\text{corr}}/i_{\text{corr}}) \times 100\% \quad (1)$$

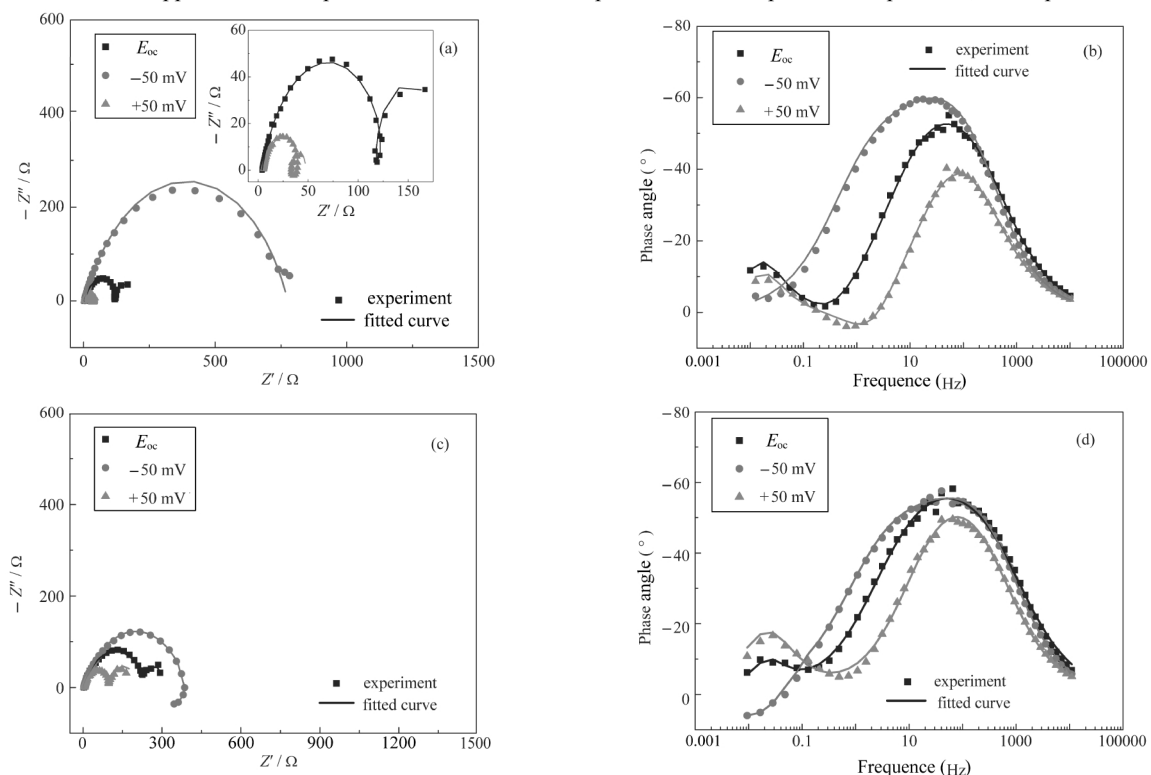
where, i_{corr} stands for the corrosion rate without dodecylamine and i'_{corr} stands for the corrosion rate with dodecylamine.

From the polarization curves (Fig. 1), it is observed that the inhibition performance of dodecylamine on N80 steel is dependent on pH value and the inhibition efficiency increases with the increase of pH value. At pH 4.9, it was easy to desorb completely for dodecylamine. The fitted data show that the addition of dodecylamine reduces the apparent Tafel slope of the anode branch

and enlarged the apparent Tafel slope of the cathode one. At pH 6.9, the addition of dodecylamine increases the apparent Tafel slopes of both anode and cathode branches. Hence, according to the polarization curves, it was deduced that dodecylamine mainly increased the resistance of the cathode process at pH 4.9. While it both increased the resistances of the anode and cathode processes and hence inhibited the anode and cathode processes at pH 6.9.

2.2 Influence of pH value on the cathode and anode processes of N80 steel corrosion

The EIS plots of N80 electrode at pH 4.9 and 6.9 in CO₂-saturated 3% NaCl solution at E_{oc} -50 mV (*vs* E_{oc}), and +50 mV (*vs* E_{oc}), are shown in Figs.2(a-d). It is observed that the characteristics of the EIS plots at the open circuit potential and the anode polarization potential at pH 4.9 (Figs.2(a,b)) are the same, while the characteristics of the EIS plots at the cathode polarization potential are different. The characteristics of the EIS plots at cathode polarization potential appeared one large and depressed capacitive loop. The broadened and slight asymmetry in the Bode plot was indicative of a second time constant^[6,7]. The capacitive loop in the high frequency was associated with the charge transfer process while the capacitive loop in the low frequency might be related to the adsorption and diffusion processes of H₂CO₃, H⁺, and HCO₃⁻ which were involved in the cathode reaction^[8]. The constant phase element (CPE) with frequency dispersion behavior^[9] was used at pH 4.9 and 6.9. The corresponding equivalent circuit is described in Fig.3(a). As to the characteristics of the EIS plots at the anode polarization potential, one depressed inductive

**Fig.2** EIS plots of N80 electrode in CO₂-saturated 3% NaCl solution without dodecylamine at different pH values

(a, b) pH=4.9; (c, d) pH=6.9

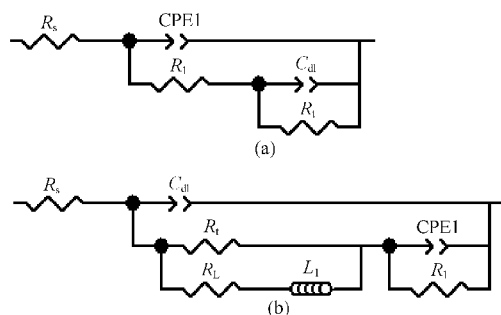


Fig.3 Equivalent circuits used to represent the electrochemical process on N80 electrode in CO₂-saturated 3% NaCl solution without dodecylamine

R_s is the solution resistance; R_f and CPE1 are the film resistance and capacitance, respectively; R_t and C_{dl} are the charge transfer resistance and the double-layer capacitance, respectively; R_i and L_1 are the resistance and the inductance related to the adsorption and desorption of the intermediates on the metal surface, respectively.

loop appeared in the middle frequency besides two capacitive loops in the high and low frequencies. The corresponding equivalent circuit is described in Fig.3 (b). The EIS plots at the open circuit potential are the coupling of the cathode and anode processes and in this case it mainly reflects the characteristics of the anode process. The equivalent circuit of Fig.3(b) is adopted to describe the electrochemical behavior at the open circuit potential.

At pH 6.9, the characteristics of the EIS plots at the open circuit potential and the anode polarization potential were the

Table 3 Fitted parameters for N80 electrode at different pH values in CO₂-saturated 3% NaCl solution without dodecylamine

pH	E/mV (vs E_{oc})	R_t/Ω	$C_{dl-T}(\mu F \cdot cm^{-2})$	C_{dl-P}
4.9	-50	745	556	0.74
	0	140	392	0.89
	+50	32	257	0.95
6.9	-50	406	797	0.68
	0	235	503	0.76
	+50	100	347	0.81

C_{dl-T} and C_{dl-P} are the capacitance and dispersion exponent, respectively.

same, while the characteristics of the EIS plots at the cathode polarization potential were different. Comparing to the EIS plots at pH 4.9, the characteristics of the EIS plots of the cathode and anode processes were obviously different and all appeared as two capacitive loops, and the inductive one appeared in the EIS plots at the anode polarization potential. The main fitted parameters are listed in Table 3.

It can be observed from the fitted results that R_t at the open circuit potential increased near one time with the increase of pH value which might be related with the protective corrosion product film formed on the metal surface. It was observed from the electrochemical plots in the uninhibited solution that the capacitive loop became flat at pH 6.9 which was explained by Mansfield *et al.*^[10] as the formation of the unhomogenous 3-D film on the metal surface. It was observed from the fitted results at cathode and anode polarization potentials that R_t of the cathode

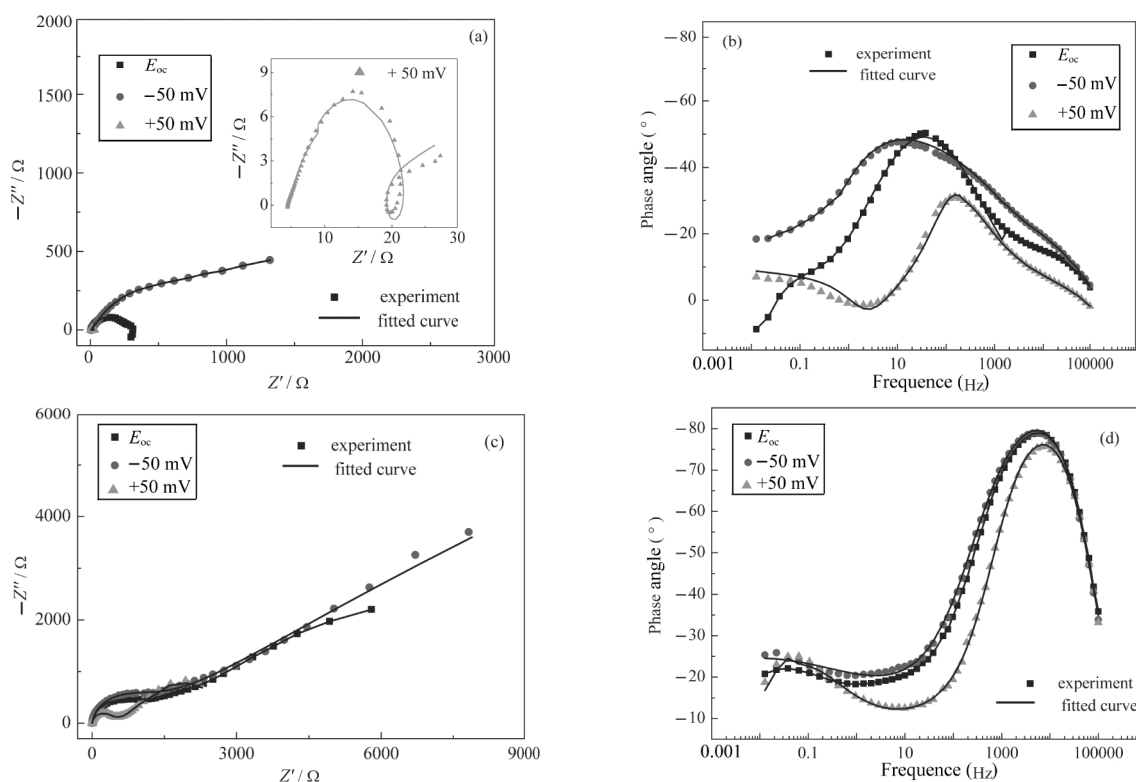


Fig.4 EIS plots of N80 electrode in CO₂-saturated 3% NaCl solution with dodecylamine

(a, b) pH=4.9, 0.65 mmol·L⁻¹ dodecylamine; (c, d) pH=6.9, 0.43 mmol·L⁻¹ dodecylamine

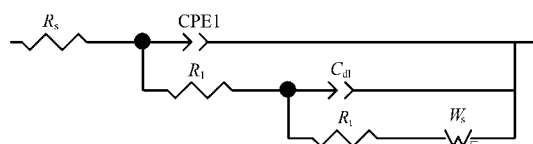


Fig.5 Equivalent circuits used to fit the EIS plot of N80 electrode in CO₂-saturated 3% NaCl solution with dodecylamine at pH 6.9

W_s is the diffusion impedance related to the diffusion layer on the metal surface.

process reduced with the increase of pH value, while the corresponding R_t at the anode process increased with the increase of pH value.

The EIS plots of N80 electrode at pH 4.9 in CO₂-saturated 3% NaCl solution at the open circuit and polarization potentials with 0.65 mmol·L⁻¹ dodecylamine are shown in Figs.4 (a, b). The characteristics of the relative EIS plots at the anode polarization potential were totally consistent with those in the absence of dodecylamine. Obvious inductive element in the EIS plot at the open circuit and polarization potentials indicated that the inhibitor was inclined to desorb. The EIS plot at the cathode polarization potential was one capacitive loop and the broadened and slight asymmetry in the corresponding Bode plot indicated the existence of two time constants. One distorted diffusion-like impedance appeared in the low frequency. The EIS plots of N80 electrode at pH 6.9 in CO₂-saturated 3% NaCl solution at the open circuit and polarization potentials with 0.43 mmol·L⁻¹ dodecylamine are shown in Fig.4s(c, d). In the presence of dodecylamine, there was an obvious change in the EIS plots and all had the characteristics of diffusion impedance.

The equivalent circuit of Fig.5 is used to describe the corrosion process on the electrode surface. The element in the high frequency (CPE1// R_1) was related to the adsorption film formed on the metal surface, the one in the middle frequency (C_{dl} // R_t) was related to the charge transfer process and the diffusion impedance element (W_s) was related to the diffusion layer on the metal surface. The main electrochemical parameters are listed in Table 4.

It was observed from the fitted results that R_t of the cathode and anode processes increased near 2–3 times compared to those without dodecylamine. Besides, the very low double-layer capacitance and the film capacitance values also indicated that

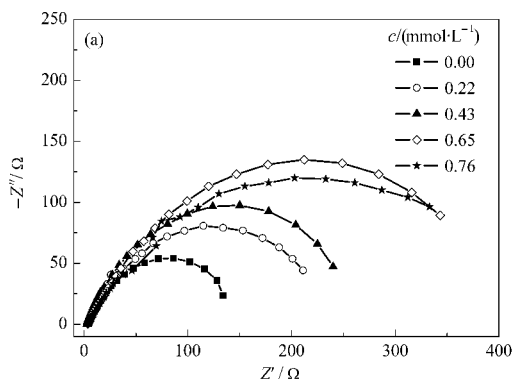


Table 4 Fitted parameters of the impedance plots in CO₂-saturated 3% NaCl solution at various pH values with dodecylamine

pH	E/mV (vs E_{oc})	R_t/Ω	$\frac{C_{dl}-T}{(\mu F \cdot cm^{-2})}$	$C_{dl}-P$	R_t/Ω	$\frac{CPE1-T}{(\mu F \cdot cm^{-2})}$	CPE1-P	f_a or f_c
4.9	-50	1383	641	0.60	-	-	-	0.53
	0	329	463	0.72	-	-	-	-
	+50	18	255	0.88	-	-	-	1.67
6.9	-50	1314	2.0	0.88	429	0.68	0.99	0.31
	0	1092	2.2	0.88	405	0.72	0.99	-
	+50	481	2.2	0.88	256	0.71	0.99	0.21

CPE1-T and CPE1-P are the capacitance and dispersion exponent, respectively; f_a and f_c are the effect coefficients to the anode and cathode of N80 steel.

water molecules at the electrode interface were largely replaced by organic inhibitor molecules. Due to the low dielectric constant of the inhibitor, the capacitance value was reduced dramatically^[11]. Dodecylamine adsorbed on the metal surface tightly and formed the dense diffusion barrier and hence reduced the corrosion processes effectively.

According to the definition of the effect coefficient of the inhibitor to the anode and cathode processes by Cao^[12], R_c which is inverse ratio to the corrosion rate, is used to calculate the effect coefficient of dodecylamine at pH 4.9 and 6.9 in the presence of dodecylamine and the obtained results are shown in Table 4. It was observed that the effect coefficient to the cathode (f_c) was smaller than that to the anode (f_a) at pH 4.9, and f_a and f_c were comparatively close at pH 6.9. It was deduced that dodecylamine mainly inhibited the cathode process of the corrosion at pH 4.9 and it inhibited the anode and cathode processes at pH 6.9.

2.3 Influence of pH value on the adsorption energy of dodecylamine

The coverage degree (θ) of the inhibitor on the metal surface is a very important parameter for the investigation of the adsorption behavior. If the inhibition efficiency (η) is instead of θ ^[13], θ can be calculated according to Formula (2):

$$\theta = 1 - R_0/R_t \quad (2)$$

where, R_0 stands for the charge transfer resistance without dodecylamine and R_t stands for the charge transfer resistance with dodecylamine. R_t was obtained according to the EIS plots at differ-

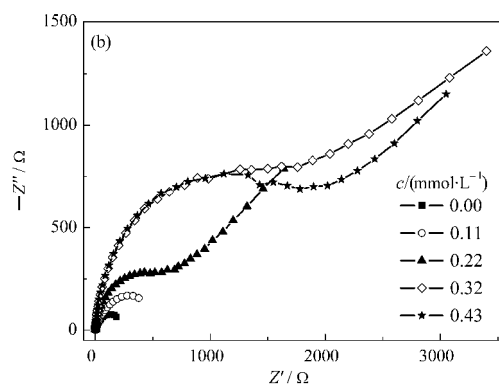


Fig.6 EIS spectra of N80 electrode in CO₂-saturated 3% NaCl solution at different concentrations of dodecylamine

(a) pH=4.9; (b) pH=6.9

Table 5 R_i and surface coverage (θ) of N80 electrode in CO_2 -saturated 3% NaCl solution with different concentrations of dodecylamine

$c/(\text{mmol}\cdot\text{L}^{-1})$	pH=4.9		pH=6.9	
	R_i/Ω	θ	R_i/Ω	θ
0.00	137	–	231	–
0.11	–	–	477	0.516
0.22	230	0.404	787	0.706
0.32	–	–	2711	0.914
0.43	290	0.528	2540	0.909
0.65	390	0.649	–	–
0.76	411	0.667	–	–

ent concentrations of dodecylamine (seen in Fig.6, the frequency range was 10 kHz–1 Hz because the aim of EIS measurement was to obtain R_i). The equivalent circuit of Fig.3(a) is used to obtain R_i , and the results are listed in Table 5. The results of the measured and the fitted are seen in Fig.7.

It was assumed that the adsorption of dodecylamine on N80 steel obeyed Freundlich isotherm. The relation of θ – c is seen in Formula (3):

$$\lg\theta = \lg K_{\text{ad}} + n \lg c \quad (3)$$

where K_{ad} is the adsorption equilibrium constant, n is the correction coefficient and c is the concentration of dodecylamine. The thermodynamic property of the adsorption energy:

$$\Delta G_{\text{ad}} = -RT \ln K_{\text{ad}} \quad (4)$$

where R is the gas constant ($8.314 \text{ J}\cdot\text{mol}^{-1}\cdot\text{K}^{-1}$) and T is the absolute temperature (K). In combination with Formulas (3) and (4), the adsorption energies of dodecylamine calculated at pH 4.9 and 6.9 were -6.9 and $-12.1 \text{ kJ}\cdot\text{mol}^{-1}$, respectively. It was observed that the adsorption energy (ΔG_{ad}) was negative at the both pH values, which indicated that the adsorption of dodecylamine on N80 steel occurred spontaneously. The adsorption energy of dodecylamine at pH 6.9 was higher than that at pH 4.9. In the aqueous solution, the dissolution equilibrium of dodecylamine existed as Formula (5):



At pH 4.9, the concentration of H^+ in the solution was higher and the equilibrium shifted to the right and the main form of dodecylamine was the protonated. At pH 6.9, the concentration of H^+ reduced. The dissolution equilibrium shifted to the left and the main form of dodecylamine was the unprotonated. The abili-

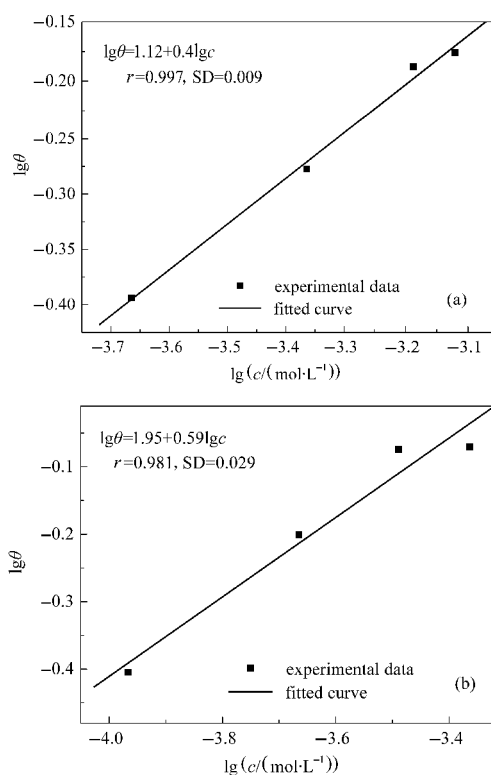


Fig.7 Fitted results of $\lg\theta$ – $\lg c$ according to Freundlich isotherm

(a) pH=4.9; (b) pH=6.9; r is the correlation coefficient; SD is the standard derivation.

ty of the inhibitor to provide the corrosion protection depends to a large extent upon the interactions between the inhibitor and the metal surface under the corrosion condition [14]. The higher electron cloud density of the nitrogen atom of dodecylamine in the molecule state compared to that in the protonated state made the inhibitor have stronger coordination ability with “ d ” orbital of the metal atom and hence had much larger adsorption ability and stability at pH 6.9.

2.4 Influence of pH value on the metal surface morphology

The surface morphologies of N80 steel exposed to CO_2 -saturated 3% NaCl solution without or with dodecylamine are shown in Fig.8 which revealed various corrosion features of the metal surface. At pH 4.9, obvious uniform corrosion is observed (Fig.8(a)).

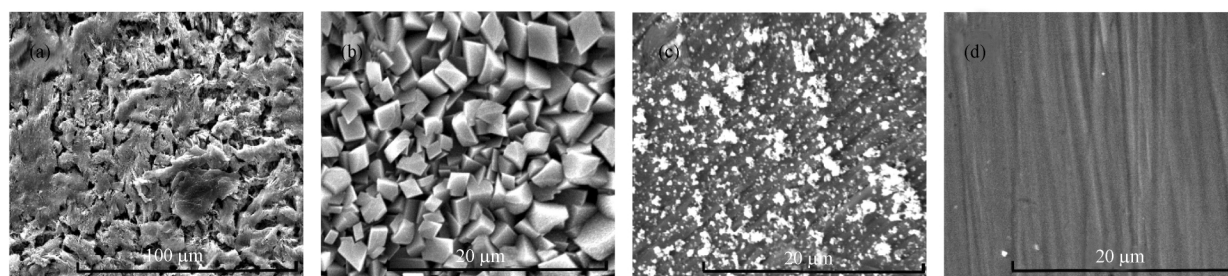


Fig.8 Surface morphologies of N80 steel after 24 h immersion in CO_2 -saturated 3% NaCl solution without or with dodecylamine

(a) pH=4.9, blank; (b) pH=6.9, blank; (c) pH=4.9, $0.65 \text{ mmol}\cdot\text{L}^{-1}$ dodecylamine; (d) pH=6.9, $0.43 \text{ mmol}\cdot\text{L}^{-1}$ dodecylamine

At pH 6.9, complete corrosion product film composed mainly of FeCO_3 is observed on the metal surface (Fig.8(b)).

In the presence of dodecylamine, the morphologies of the metal surface changed obviously. At pH 4.9, many corrosion products were still observed on the metal surface (Fig.8(c)) which well corroborated that dodecylamine did not provide effective inhibition. With the increase in pH value, the addition of dodecylamine basically inhibited the formation of the corrosion products. Not only were the large amounts of FeCO_3 -like corrosion products not observed, but also the polished naked metal morphology with the nicks was distinguished obviously (Fig.8(d)). The difference of the morphology of the metal surface might be ascribed to the effective adsorption of the inhibitor on the metal surface which formed the hydrophobic barrier and hence reduced the corrosion rate of N80 steel.

3 Conclusions

(1) The inhibition performance of dodecylamine on N80 steel was dependent on pH value and the inhibition efficiency increased with the increase of pH value. At pH 4.9, the adsorption energy of dodecylamine on the metal surface was lower, and the desorption of the inhibitor was easy to occur. Hence, dodecylamine did not inhibit effectively the corrosion process. At pH 6.9, the adsorption energy of dodecylamine was higher, and it adsorbed on the metal surface tightly. The formation of the effective diffusion barrier provided excellent inhibition ability.

(2) At pH 4.9, dodecylamine mainly increased the resistance of the cathode process and hence inhibited mainly the cathode process of the corrosion. At pH 6.9, dodecylamine increased the resistances of both cathode and anode processes and hence in-

hibited the cathode and anode processes of the corrosion.

References

- 1 Jovancevic, V.; Ramachandran, S.; Prince, P. *Corrosion*, **1999**, **55**: 449
- 2 Mora-Mendoza, J. L.; Turgoose, S. *Corrosion Science*, **2002**, **44**: 1223
- 3 Hernandez, S.; Vera, J. R. *NACE: Corrosion*, **1998**: paper no23
- 4 Moiseeva, L. S.; Rashevskaya, N. S. *Russian Journal of Applied Chemistry*, **2002**, **75**: 1625
- 5 Altoe, P.; Pimenta, G.; Moulin, C. F.; Diaz, S. L.; Mattos, O. R. *Electrochimica Acta*, **1996**, **41**: 1165
- 6 de Marco, R.; Durnie, W.; Jefferson, A.; Kinsella, B.; Crawford, A. *Corrosion*, **2002**, **58**: 354
- 7 Villamizar, W.; Casales, M.; Gonzales-Rodriguez, J. G.; Martinez, L. *Materials and Corrosion*, **2006**, **57**: 696
- 8 Fan, Z. H.; Lü, X. H.; Zhao, G. X.; Lu, M. X. *Corrosion Science and Protection Technology*, **2005**, **17**: 75 [樊治海, 吕祥鸿, 赵国仙, 路民旭. 腐蚀科学与防护技术, **2005**, **17**: 75]
- 9 Popova, A.; Sokolova, E.; Raicheva, S. *Corrosion Science*, **2003**, **45**: 33
- 10 Mansfeld, F.; Kendig, M. W.; Lorenz, W. J. *Journal of the Electrochemical Society*, **1985**, **132**: 290
- 11 Tan, Y. J.; Bailey, S.; Kinsella, B. *Corrosion Science*, **1996**, **38**: 1545
- 12 Cao, C. N. *Corrosion electrochemistry*. Beijing: Chemical Industry Press, 1994: 128-129 [曹楚南. 腐蚀电化学. 北京: 化学工业出版社, 1994: 128-129]
- 13 Gasparac, R.; Stupnisek-Lisac, E. *Corrosion*, **1999**, **55**: 1031
- 14 Li, P.; Lin, J. Y.; Tan, K. L.; Lee, J. Y. *Electrochimica Acta*, **1997**, **42**: 605